Inherited human cPLA$_{2\alpha}$ deficiency is associated with impaired eicosanoid biosynthesis, small intestinal ulceration, and platelet dysfunction

David H. Adler,[1] Joy D. Cogan,[2] John A. Phillips III,[2] Nathalie Schnetz-Boutaud,[3] Ginger L. Milne,[1] Tina Iverson,[4] Jeffrey A. Stein,[5] David A. Brenner,[5] Jason D. Morrow,[1] Olivier Boutaud,[1] and John A. Oates[1]

[1]Departments of Medicine and Pharmacology, Division of Clinical Pharmacology, Vanderbilt University Medical Center, Nashville, Tennessee, USA. [2]Department of Pediatrics, Division of Medical Genetics, Vanderbilt University Medical Center, Nashville, Tennessee, USA. [3]Center for Human Genetics Research, Vanderbilt University Medical Center, Nashville, Tennessee, USA. [4]Department of Pharmacology, Vanderbilt University Medical Center, Nashville, Tennessee, USA. [5]Department of Medicine, Division of Digestive and Liver Diseases, Columbia University Medical Center, New York, New York, USA.

Cytosolic phospholipase A$_{2\alpha}$ (cPLA$_{2\alpha}$) hydrolyzes arachidonic acid from cellular membrane phospholipids, thereby providing enzymatic substrates for the synthesis of eicosanoids, such as prostaglandins and leukotrienes. Considerable understanding of cPLA$_{2\alpha}$ function has been derived from investigations of the enzyme and from cPLA$_{2\alpha}$-null mice, but knowledge of discrete roles for this enzyme in humans is limited. We investigated a patient hypothesized to have an inherited prostanoid biosynthesis deficiency due to his multiple, complicated small intestinal ulcers despite no use of cyclooxygenase inhibitors. Levels of thromboxane B$_2$ and 12-hydroxyeicosatetraenoic acid produced by platelets and leukotriene B$_4$ released from calcium ionophore–activated blood were markedly reduced, indicating defective enzymatic release of the arachidonic acid substrate for the corresponding cyclooxygenase and lipoxygenases. Platelet aggregation and degranulation induced by adenosine diphosphate or collagen were diminished but were normal in response to arachidonic acid. Two heterozygous single base pair mutations and a known SNP were found in the coding regions of the patient's cPLA$_{2\alpha}$ genes (p.[Ser111Pro]+[Arg485His; Lys651Arg]). The total PLA$_2$ activity in sonicated platelets was diminished, and the urinary metabolites of prostacyclin, prostaglandin E$_2$, prostaglandin D$_2$, and thromboxane A$_2$ were also reduced. These findings characterize what we believe is a novel inherited deficiency of cPLA$_2$.

Introduction

These investigations addressed the problem of a patient with multiple small intestinal ulcers that were not associated with use of NSAIDs. The patient had chronic gastrointestinal blood loss from childhood with no source identified by repeated esophagogastroduodenal and colonic endoscopies until the fourth decade, when multiple small intestinal ulcers were discovered in the context of severe bleeding and perforations. The etiology of small intestinal ulcers previously reported to occur independently of NSAIDs and enteric-coated drugs (1) had not been elucidated, and these ulcers had been designated as "idiopathic."

Evidence from both experimental animals and humans has demonstrated that drugs that inhibit both the COX-1 and COX-2 pathways of PG biosynthesis will produce ulcers of the small intestine (2–5). This evidence led us to hypothesize that the NSAID-independent small bowel ulcers in this patient could be due to a genetic defect in PG biosynthesis or signaling.

The patient was found to have a global reduction in eicosanoid biosynthesis. After excluding a COX-1 deficiency, the investigation led to the discovery of a compound heterozygous mutation of the cytosolic phospholipase A$_{2\alpha}$ (cPLA$_{2\alpha}$) gene (*PLA2G4A*) with loss of cPLA$_{2\alpha}$ function. cPLA$_{2\alpha}$ is a calcium-activated phospholipase that, by liberation of arachidonic acid (AA) from phospholipids, functions as a rate-limiting step in the biosynthesis of eicosanoids (Figure 1).

Results

Clinical presentation. The proband is a 45-year-old white American male of Italian descent with a life-long history of occult gastrointestinal blood loss, chronic anemia, iron deficiency, and frequent bouts of abdominal pain as a child and young adult. Repeated episodes of acute gross gastrointestinal bleeding late in his fourth decade and multiple episodes of small bowel perforation required 5 surgical interventions between 38 and 45 years of age. Surgical exploration of the small intestine and intraoperative endoscopy revealed multiple recurrent ulcerations. Histologic specimens of the ileum and jejunum revealed multiple small, well-demarcated ulcers with minimal surrounding inflammation (Figure 2). Stenotic ileal web formations were also described proximal to several

Nonstandard abbreviations used: AA, arachidonic acid; ACN, acetonitrile; ADP, adenosine diphosphate; ATP, adenosine triphosphate; cPLA$_{2\alpha}$, cytosolic phospholipase A$_{2\alpha}$; 11-dTxB$_2$, 11-dehydrothromboxane B$_2$; ECI, electron capture ionization; GC, gas chromatography; 12-HETE, 12-hydroxyeicosatetraenoic acid; LC, liquid chromatography; LTE$_4$, leukotriene E$_4$; M, metabolite(s); MS, mass spectrometry; PGD$_2$, prostaglandin D$_2$; PGI$_2$, prostacyclin; PIP$_2$, phosphatidylinositol 4,5-bisphosphate; PRP, platelet-rich plasma; TxA$_2$, thromboxane A$_2$.

Conflict of interest: The authors have declared that no conflict of interest exists.

Citation for this article: *J. Clin. Invest.* **118**:2121–2131 (2008). doi:10.1172/JCI30473.

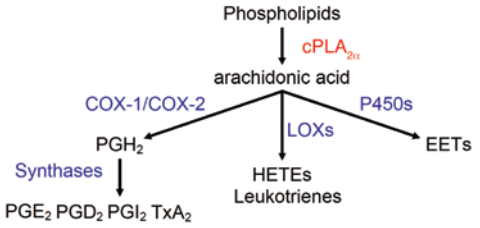

Figure 1
Arachidonic cascade initiated by $cPLA_{2\alpha}$. P450, cytochrome P450; LOX, lipoxygenase. $cPLA_{2\alpha}$ reaction is in red, and other enzymatic reactions are in blue.

ulcers. Misoprostol (800 μg daily), an oral prostaglandin E_1 (PGE_1) analog, had been initiated within the year prior to evaluation with subsequent resolution of anemia for a period of 27 months until gastrointestinal bleeding recurred again.

Colonoscopy and esophagogastroduodenoscopy had been performed on multiple occasions and always had been normal. Mesenteric arteriograms, gastrin secretion, and laboratory and histologic evaluation for celiac sprue and inflammatory bowel disease were all normal. He denied having had diarrhea, nausea, vomiting, or constipation. He had no history of bruising or nongastrointestinal bleeding symptoms or severe or recurrent infections.

A cystic renal mass, detected at age 38 and resected at age 40, revealed a clear cell renal carcinoma (Furman grade II). A brief period of mild wheezing in early childhood was reported without subsequent respiratory complaints. A shellfish allergy causing urticaria was reported. Medications included iron sulfate and a multivitamin in addition to misoprostol. Use of nonsteroidal antiinflammatory and corticosteroid medications was specifically denied.

The patient had a brief and remote history of smoking and consumed only moderate amounts of alcohol. His father had died with multiple myeloma, and varying malignancies were reported in second- and third-degree relatives. No renal malignancy was reported in family members. There was no family history of ulcers. Two cousins had reported gastrointestinal blood loss and, after further exploration, were deemed to have symptoms of an unrelated etiology. Both of these relatives (a father and son) were genotyped and did not have any of the $cPLA_{2\alpha}$ transitions described later in this text. One was further evaluated as an inpatient at the Clinical Research Center at Vanderbilt University Medical Center. His symptoms differed significantly from the proband; he did not have ulcers on video capsule endoscopy, and he exhibited normal platelet function.

Physical examination revealed a well-developed male. Blood pressure was normal. A 2/6 systolic murmur was heard at the left sternal border. His abdomen was notable for multiple well-healed surgical scars. Physical examination was otherwise unremarkable.

An electrocardiogram and an echocardiogram were normal. Ultrasonography demonstrated normal kidneys with evidence of prior partial resection. Blood cell counts, electrolytes, and renal and liver function values were normal (Table 1).

A systemic deficiency in eicosanoid production is demonstrated by reduction in urinary metabolites of PGE_2, PGD_2, prostacyclin (PGI_2), and thromboxane A_2 (TxA_2). Urinary metabolites (M) of TxA_2 (11-dehydrothromboxane B_2 [11-dTxB_2]), PGI_2 (2,3-dinor-6-keto-$PGF_{1\alpha}$; PGI-M), PGD_2 (9α,11β-dihydroxy-15-oxo-2,3,18,19-tetranorprost-5-ene-1,20-dioic acid; PGD-M), and PGE_2 (11α-hydroxy-9,15-dioxo-2,3,4,5-tetranor-prostane-1,20-dioic acid; PGE-M) were assayed using mass spectrometry (MS). The patient's urinary prostanoid metabolites demonstrated reduced levels compared with reference values (Table 2) (6–9). The patient's mean 11-dTxB_2 was 58.7 ± 15.14 pg/mg Cr (n = 3); mean PGI-M was 53.67 ± 39.27 pg/mg Cr (n = 3); mean PGD-M was 387 ± 347 pg/mg Cr (n = 4); and mean PGE-M was 4.48 ± 1.65 ng/mg Cr (n = 3). The patient's mother and sister did not have reduced urinary prostanoid metabolite levels (Table 2).

Platelet-derived (serum) TxB_2 and 12-hydroxyeicosatetraenoic acid (12-HETE) were markedly reduced, suggesting a deficiency

Table 1
Baseline laboratory values

Lab test	Patient	Reference range
White blood count	6.1	3.9–10.3 (10^3/μl)
Hemoglobin	14.7	14.0–18.0 (g/dl)
Hematocrit	43	42–50 (%)
Mean corpuscular volume	87	83–102 (fl)
Neutrophils	71.0	36.0–74.0 (%)
Lymphocytes	19.7	27.0–43.0 (%)
Monocytes	6.0	3.0–11.0 (%)
Eosinophils	3.0	0.1–5.0 (%)
Platelets	142	135–370 (10^3/μl)
Sodium	140	135–145 (mEq/l)
Potassium	4.4	3.5–5.1 (mEq/l)
Chloride	109	95–105 (mEq/l)
Carbon dioxide	23	23–30 (mmol/l)
Blood urea nitrogen	21	5–25 (mg/dl)
Creatinine	1.0	0.7–1.5 (mg/dl)
Glucose	90	70–110 (mg/dl)
Calcium	9.1	8.5–10.5 (mg/dl)
Albumin	4.2	3.5–5.0 (g/l)
Total protein	6.9	6.0–8.0 (g/dl)
Total bilirubin	0.3	0.2–1.2 (mg/dl)
Alkaline phosphatase	48	40–110 (U/l)
AST	20	4–40 (U/l)
ALT	46	4–40 (U/l)
Total cholesterol	110	(mg/dl)
Triglycerides	225	(mg/dl)
HDL-C	25	(mg/dl)
LDL-C	40	(mg/dl)
Hemoglobin $A1_C$	4.2	(%)
Ferritin	22	10–300 (ng/ml)
Urine creatinine	1.97	1.0–2.0 (g/l)
Glomerular filtration rate	134.1	(ml/min/1.73 m^2)
Urine sodium	120	80–180 (mEq/l)
Urine potassium	70.0	40–80 (mEq/l)
Urine chloride	113	110–250 (mEq/l)
Urine calcium	122	50–150 (mg/l)
Urine osmolality	858	300–1100 (mosm/kg H_2O)
Urine methylhistamine	138	50–230 (μg/g creatinine)
Renin (supine)	0.5	0.3–1.7 (ng/ml)
Renin (upright)	0.9	0.7–3.3 (ng/ml)
Aldosterone (supine)	5.0	1–16 (ng/dl)
Aldosterone (upright)	5.2	4–31 (ng/dl)

Analyzed by the Clinical Pathology Laboratory at Vanderbilt University Medical Center. HDL-C, HDL cholesterol; LDL-C, LDL cholesterol; AST, aspartate transaminase; ALT, alanine transaminase.

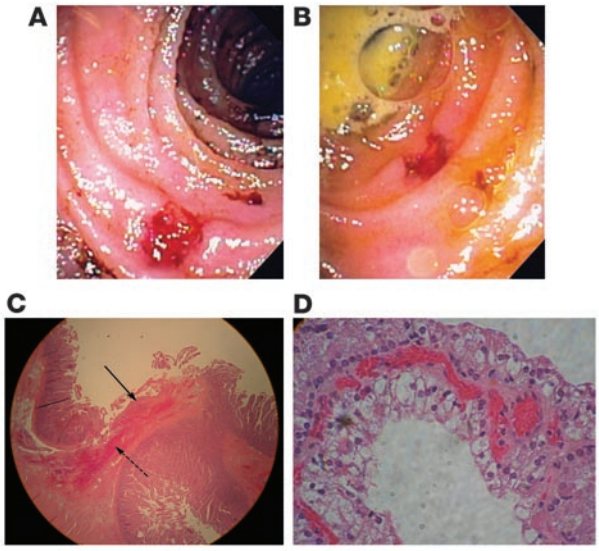

Figure 2
Gross and histologic pathology. (**A** and **B**) Intraoperative endoscopy shows a well-demarcated ulcer in the proximal ileum with minimal surrounding inflammation. (**C**) A shallow jejunal ulcer involves the mucosa and submucosa. Acute inflammatory exudate covers the ulcer base (solid arrow). Neutrophils infiltrate the submucosa (dashed arrow). There are no signs of chronicity nor evidence of viral inclusion, inflammatory bowel disease, or vasculitis. Original magnification, ×100. (**D**) Renal-cell carcinoma, Furman grade II. Original magnification, ×100.

in biosynthesis proximal to COX-1 and 12-lipoxygenase. The finding that 11d-TxB_2 excretion was reduced by 84.1% led to the hypothesis that TxA_2 biosynthesis by the platelet was impaired. This was assessed by measurement of TxB_2 released into the serum during blood clotting, which is derived almost entirely from platelets (10). The patient's mean serum TxB_2 was reduced by 95.9% compared with controls (n = 49; Figure 3). This could reflect pharmacologic inhibition of platelet COX-1, COX-1 deficiency, or lack of the COX-1 substrate AA. A genetic deficiency of thromboxane synthase seemed unlikely due to the depressed biosynthesis of other prostanoids. To distinguish between these possibilities, the product of the platelet 12-lipoxygenase, 12-HETE, was measured in serum; 12-HETE should be unchanged or increased with pharmacologic or genetic impairment of COX-1 catalytic activity. The level of 12-HETE in the patient's serum was decreased by 97.8% compared with controls (n = 42; Figure 3), a finding consistent with an almost complete absence of the release of AA during platelet activation (Figure 1). The patient's mother and sister exhibited intermediate values for platelet-derived TxB_2 and 12-HETE that were below or at the lower end of the normal range (Figure 3).

COX-1 activity in the patient's platelets was normal. COX-1 activity was assessed by measuring production of TxA_2 by washed platelets after incubation with [$^2H_8$] AA (Figure 4). Both deuterated and nondeuterated TxB_2 were quantified, reflecting conversion by COX-1 of exogenous and endogenous substrate, respectively. [$^2H_8$] TxB_2 levels were similar between the patient and controls, reflecting normal COX-1 activity in the patient's platelets. Platelet activation by exogenous agonists, including AA, induces release of endogenous AA from cellular storage pools. Notably, nondeuterated TxB_2 levels from the patient's platelets were much lower than those of controls (0.04 vs. 0.51 ng/10^3 platelets; n = 1), indicating an impaired release of endogenous AA.

Platelet function was impaired in response to adenosine diphosphate and collagen but normal in response to AA. Platelet function was assessed by monitoring platelet aggregation and dense granule secretion in response to stimulation by adenosine diphosphate (ADP) or collagen (Figure 5). ADP (5 μM) and collagen (2 μg/ml) were the lowest doses of these reagents inducing granule secretion in all controls. ADP (5 μM) induced a diminished aggregation of the patient's platelets compared with that in controls (n = 6; mean 73.0 ± 8.29 vs. 92.67 ± 11.91 maximum percentage of aggregation; $P < 0.005$). Collagen (2 μg/ml) also induced less aggregation in the patient, inducing a mean percentage of maximal aggregation of 61.0 ± 14.8 vs. 95.33 ± 15.2 in controls ($P < 0.005$). Notably, adenosine triphosphate (ATP) release, which is a measure of dense granule secretion, in response to ADP was completely absent in the patient's platelets

Table 2
Eicosanoid metabolites

Leukocyte-derived eicosanoids	Patient	Reference range	Patient vs. normal mean (%)	Mother	Sister
LTB_4 (ng/ml)	7.2 ± 3.3	223–271	2.96%	NA	NA
Urinary eicosanoid metabolites					
11-dTxB_2 (pg/mg creatinine)	58.7 ± 15.1[A]	96–644	15.9 %	319	188
PGI-M (pg/mg creatinine)	53.7 ± 39.3[A]	65.1–291.9	30.0 %	318	158
PGD-M (ng/mg creatinine)	0.39 ± 0.35[A]	0.74–1.64 (males) 0.72–1.2 (females)	32.8 %	2.40	0.86
PGE-M (ng/mg creatinine)	4.48 ± 1.65[A]	7.4–13.4 (males) 4.6–7.4 (females)	43.1 %	23.6[A]	8.6[A]
LTE_4 (pg/mg creatinine)	Undetectable	19–60		NA	NA

Urinary metabolites of TxA_2, PGI_2 (PGI-M), PGD_2 (PGD-M), and PGE_2 (PGE-M) were measured by mass spectroscopy from 24-hour urine collections. Normal values for whole-blood LTB_4 represent the mean of control volunteers ± 2 SDs. Normal values for urinary prostanoid metabolites were published previously (6–9). [A]Mean outside of reference range.

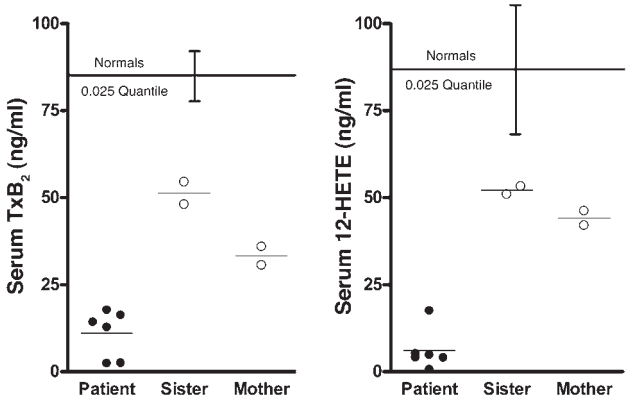

Figure 3
Platelet-derived eicosanoid biosynthesis. Serum TxB_2 was measured by GC/MS, and serum 12-HETE was measured by LC/MS. Normal values for serum eicosanoids were obtained from healthy male volunteers (n = 49 for TxB_2; n = 42 for 12-HETE). The lower limits of the reference ranges are represented by the 0.025 quantiles for normal volunteers (brackets represent 0.025 quantiles ± SEM). Mean values are represented by horizontal bars. Individual measurements are plotted for patient (closed circles) and heterozygous family members (open circles).

as opposed to in controls, which released a mean 0.88 ± 0.33 nmol ATP (P = 0.001). ATP release in response to collagen 2 (μg/ml) also was decreased significantly in the patient versus controls (mean 0.16 ± 0.032 vs. 1.1 ± 0.34 nmol; P = 0.002). Normal aggregation and ATP release were observed in the patient's platelet-rich plasma (PRP) with addition of AA (250 μM).

Levels of $cPLA_{2\alpha}$ protein in platelets were reduced. Immunoblotting for $cPLA_{2\alpha}$ in the patient's platelets detected protein of expected molecular weight but in diminished quantity (approximately 38% of control) (Figure 6A). COX-1 was detected in equal amounts in the patient and controls.

Total PLA_2 activity in platelets is reduced. The patient's mean total PLA_2 activity in sonicated platelets represented 27.2% of the activity in controls (n = 4), with mean activity of 0.77 ± 0.32 vs. 2.83 ± 0.47 pmol/min/50 μg protein (P < 0.0005) in controls (Figure 6B). PLA_2 activity in the patient's cultured lymphoblast line was 24.7% of that in controls (n = 4), with mean activity of 0.93 ± 0.098 vs. 3.77 ± 0.73 pmol/min/50 μg protein (P < 0.001).

The biosynthesis of leukotriene E_4 and leukotriene B_4 is markedly reduced. Urinary leukotriene E_4 (LTE_4) was below the limit of detection of 1 pg/ml in the patient's urine. LTB_4 produced by whole blood activated by calcium ionophore from the patient measured 7.2 ± 3.3 ng/ml whereas whole blood from healthy volunteers produced 243.7 ± 22.6 ng/ml LTB_4 (n = 2).

The patient had compound heterozygous mutations of PLA2G4A. Three transitions encoding nonsynonymous codons in the patient's $cPLA_{2\alpha}$ alleles were found by sequencing $cPLA_{2\alpha}$ cDNA derived from his total RNA. These included a T to C transition (c.[331T>C]) resulting in a TCT to CCT substitution encoding a Ser to Pro change at residue 111 (p.[S111P]), a G to A transition (c.[1454G>A]) resulting in a CGT to CAT substitution encoding an Arg to His change at residue 485 (p.[R485H]), and an A to G transition (c.[1952A>G]) resulting in an AAG to AGG substitution encoding a Lys to Arg change at residue 651 (p.[K651R]) (Figure 7A). The patient was heterozygous for all 3 transitions, and no changes were found in the 3′ or 5′ untranslated regions. Sequencing of $cPLA_{2\alpha}$ cDNA from the patient's mother and sister showed that the mother was heterozygous for the p.[S111P] variant but was homozygous for the p.[R485] and p.[K651] alleles. The sister was heterozygous for both the p.[R485H] and p.[K651R] variants but was homozygous for p.[S111] alleles. This inheritance pattern demonstrates that the patient was compound heterozygous with the p.[S111P] transition on one allele and both the p.[R4885H] and p.[K651R] transitions on the other allele. All of the variants detected in cDNA products were confirmed by direct sequencing of the corresponding segments of genomic DNA.

The detected mutations were rare. An ethnically diverse DNA panel was screened for the transitions using an allelic discrimination assay. We found no p.[S111P] or p.[R485H] alleles among the 418 DNA samples (836 alleles) screened, suggesting that p.[P111] and p.[H485] are rare, variant $cPLA_{2\alpha}$ alleles. These 2 variant alleles are also not described in the NCBI SNP database (http://www.ncbi.nlm.nih.gov/projects/SNP/). In contrast, we found 9 samples with the p.[R651] allele, all heterozygous, among the 418 samples, demonstrating an allelic frequency of 1.08% (9/836). This suggests that the p.[R651] is a SNP allele since its frequency exceeds 1% in the con-

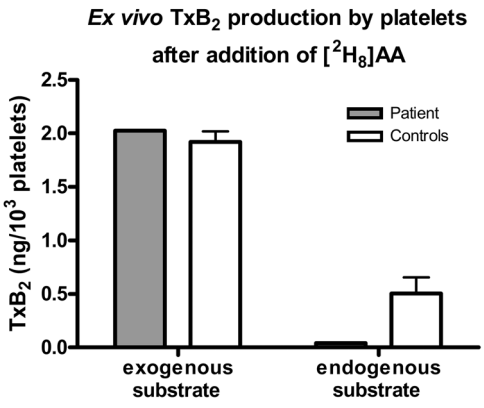

Figure 4
Ex vivo TxB_2 production by washed platelets after the addition of deuterated AA (2 μM). Endogenous substrate converted by platelet COX-1 was measured as nondeuterated TxB_2, whereas exogenous substrate was measured as deuterated TxB_2. Both deuterated and nondeuterated TxB_2 were measured simultaneously in the same samples after addition of deuterated AA to assess endogenous AA release triggered by exogenous AA. Error bars represent ± SD.

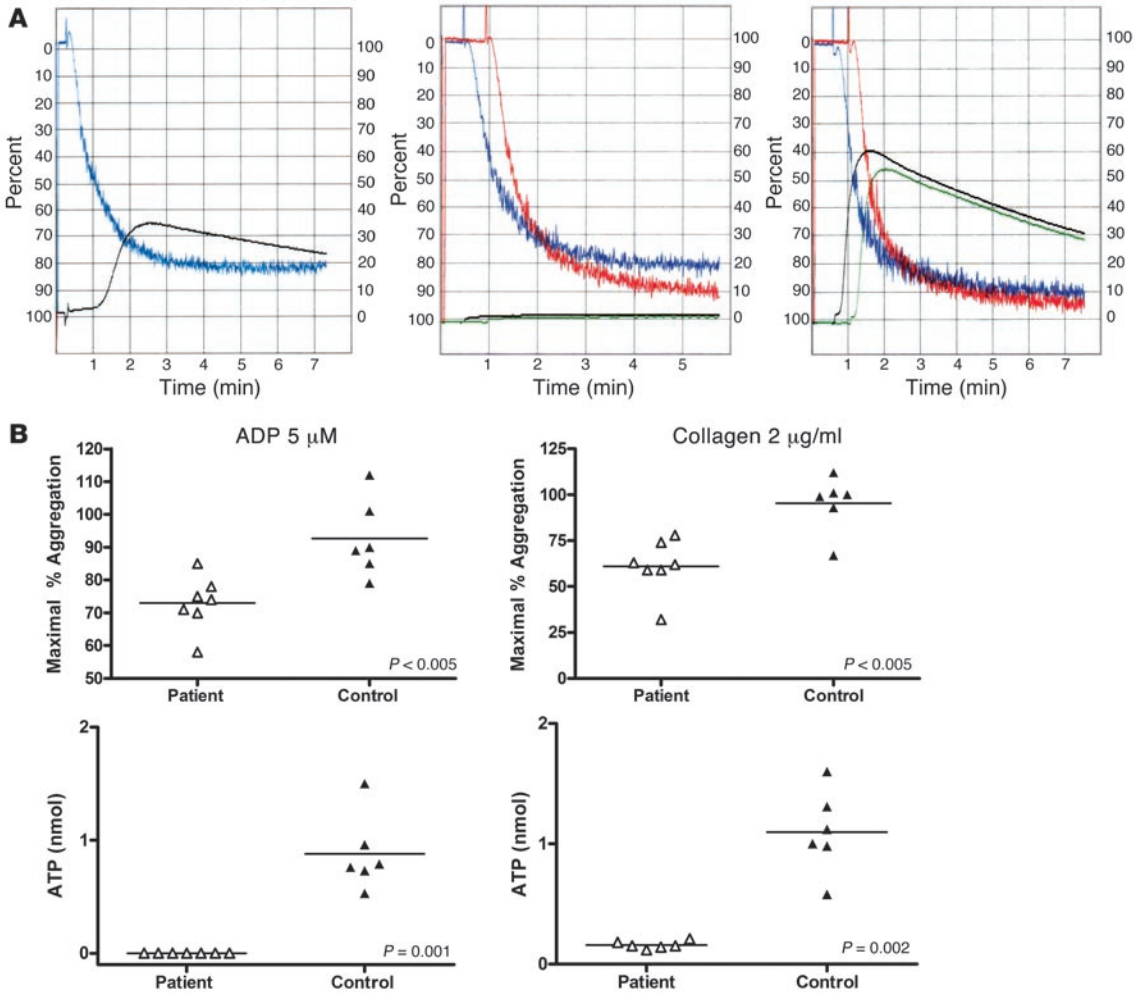

Figure 5
Platelet aggregation and dense granule release. (**A**) Representative measurements of platelet aggregation and simultaneous ATP release. Left panel shows aggregation (blue) and ATP release (black) in platelets from a normal control in response to ADP (10 μM). Middle panel shows aggregation (blue and red, performed in duplicate) and ATP release (black and green, in duplicate) in platelets from the proband in response to ADP (10 μM). Right panel shows aggregation (blue and red, in duplicate) and ATP release (black and green, in duplicate) in platelets from the proband in response to AA (500 μM). (**B**) Optical platelet aggregation in PRP in response to ADP (5 μM) or collagen (2 μg/ml) and ATP release as a measure of platelet degranulation recorded simultaneously during platelet aggregation. Each point represents 1 measurement (different days for the patient and different control volunteers); horizontal bars represent mean.

trol population. In agreement with our data, p.[K651R] has been previously recognized as a SNP in the NCBI database (rs2307198), located in the C-terminal region of the catalytic domain.

Molecular modeling suggested functional consequences of the detected mutations. The serine at position 111 normally forms a hydrogen-bonding interaction with the backbone carbonyl of the edge β-strand in the fold. The described p.[S111P] variant would substitute a proline at this position (Figure 8). When position 111 is modeled as proline, the favorable hydrogen-bonding interaction is lost and potentially unfavorable steric interactions are formed (Figure 9).

The catalytic domain contains an active site composed of the catalytic dyad p.[S228] and p.[D549] (11). In addition to these 2 amino acids, p.[R200] is also a known functionally obligate residue (Figure 8) (11). Near the active site, p.[R485] is in proximity to a cluster of lysine residues that are essential for interfacial binding of $cPLA_{2\alpha}$ (12) and for binding phosphatidylinositol 4,5-bisphosphate (PIP_2) (13). p.[R485] is located in a cleft in a helical region containing several positively charged residues in the membrane-facing region of the catalytic domain (11), where the side-chain guanido group forms 2 stabilizing hydrogen-bonding interactions within this fold. When a His is modeled into position 485, the 2 hydrogen-bonding interactions are lost, and a small destabilizing cavity would be expected to form since His has a smaller side chain (Figure 10).

Crystallographic data have not unambiguously determined the relative position of p.[K651] nor conferred information about this region that engenders a specific functional hypothesis.

Discussion

We have discovered what we believe is a novel functional deficiency of $cPLA_{2\alpha}$ resulting from compound heterozygosity for 2 rare variants (p.[S111P] and p.[R485H]) in a patient with small intestinal ulcers, platelet dysfunction, and globally decreased eicosanoid

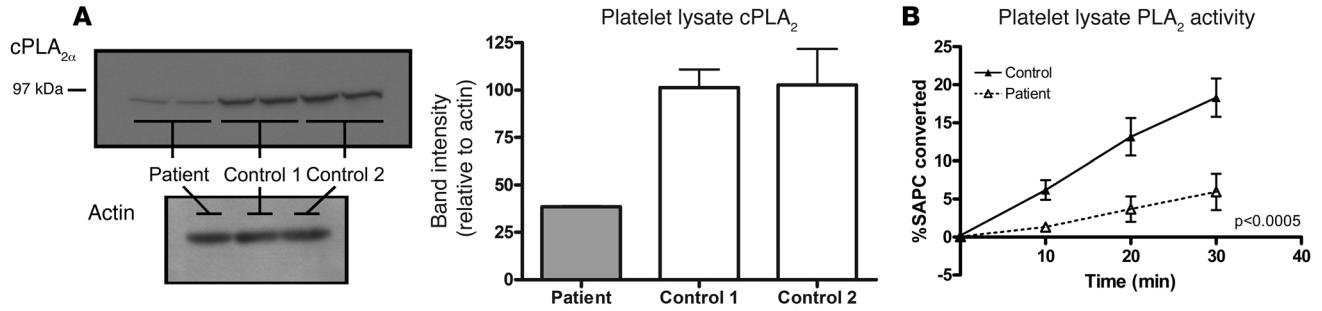

Figure 6
Platelet PLA_2 quantity and activity. (**A**) Western blot of platelet lysate from the patient demonstrates $cPLA_{2\alpha}$ protein of expected molecular weight but in diminished quantity compared with controls. Band intensity was quantified using Quantity One image analysis software ($n = 3$). Error bars represent ± SD. (**B**) PLA_2 activity in platelet lysate measured by hydrolysis of a radiolabeled substrate, l-3-phosphatidylcholine, 1-stearoyl-2-[1-^{14}C] arachidonyl (^{14}C-SAPC). Points represent mean values for each time point ($n = 4$; 2 separate experiments performed in duplicate: 2 control volunteers and 2 different collection days for patient). Error bars represent ± SD.

production. Our findings indicate that eicosanoid biosynthesis by human platelets and leukocytes is derived almost entirely via the $cPLA_{2\alpha}$ pathway and suggest that this phospholipase contributes importantly to maintaining the integrity of the small intestine.

Concerted evidence supports a causal relationship between the observed mutations and the phenotype. Both the c.[331T>C] and the c.[1454 G>A] are missense mutations. Each of these mutations is rare; neither was found in the population of 418 DNA multiethnic samples that we analyzed, and neither was reported in the NCBI SNP database. These rare mutations are associated with a rare biochemical phenotype; no evidence for a block in eicosanoid biosynthesis at the level of $cPLA_2\alpha$ has previously been reported in humans. The clinical phenotype of early onset of iron-deficiency anemia due to non–drug-related small bowel ulcers also is very uncommon. The biochemical phenotype of impaired biosynthesis of both TxB_2 and 12-HETE in platelets cosegregates with the mutations in the family, with the compound heterozygosity for the mutations in the patient yielding virtually complete absence

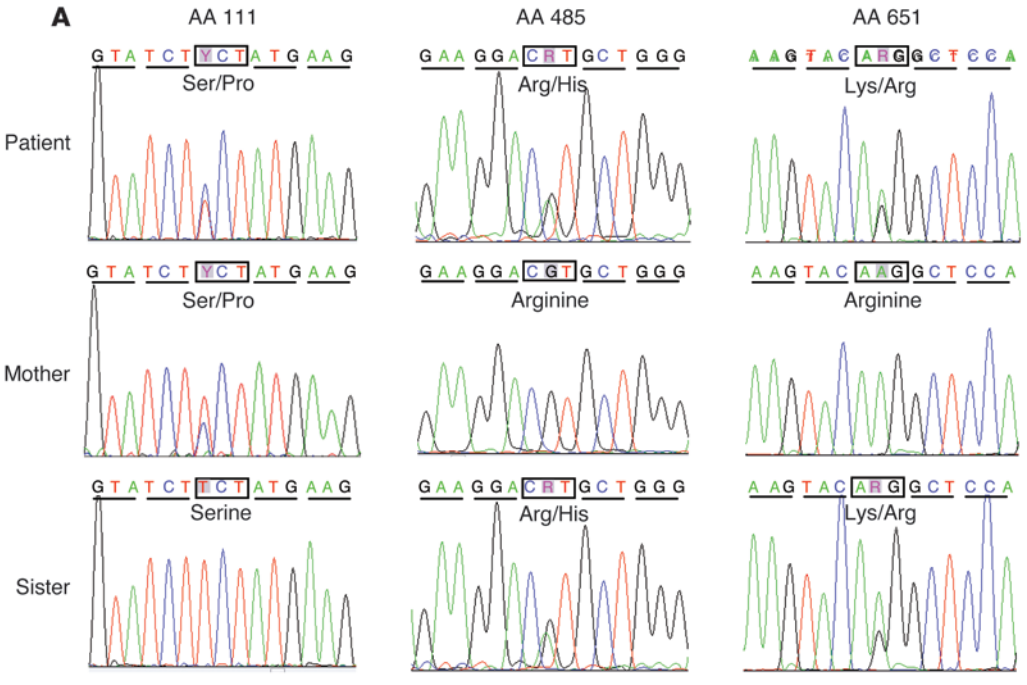

B

AA#	Ser111	AA#	Arg485	AA#	Lys651	
106	TFTVSSMKVGE	480	NTREGRAGKVH	646	NFRKYKAPGVP	*H. sapiens* (human)
106	TFPISSLKLGE	480	NTREGRAGKVH	646	NFRKYKAPGLP	*G. gallus* (chicken)
106	TFPVSSMKVGE	480	NTREGRAGKVH	646	NFRKYKAPGVL	*R. norvegicus* (rat)
165	TFPISSMRVGD	539	NTREGRAGKVH	705	NFRKYKAPGVP	*C. familiaris* (dog)
106	TFPVSSMKVGE	480	NTREGRAGKVH	645	NFRKYKAPGVL	*M. musculus* (mouse)
106	TFPILSVKPGE	480	NTREGRAGKVH	646	QFRNFKAPGVP	*X. laevis* (frog)
100	KYSLSKLKVAQ	474	TTREGRAGKVH	635	NFRNFKAPGVP	*D. rerio*(zebrafish)

Figure 7
$cPLA_{2\alpha}$ mutations. (**A**) $cPLA_{2\alpha}$ cDNA sequence chromatograms identifying 3 transitions that encode heterozygous nonsynonymous amino acid substitutions (S111P, R485H, and K651R) in a patient with $cPLA_{2\alpha}$ deficiency. The patient's mother was only heterozygous for the S111P alleles, while his sister was heterozygous for both the R485H and K651R alleles. (**B**) Sequence conservation around each amino acid substitution. Amino acid sequences from human, chicken, rat, dog, mouse, frog, and zebrafish were compared. All 3 identified amino acid changes were highly conserved across species. Sequences were obtained and aligned from the NCBI BLAST database (BLAST 2 sequences (59); blastp 2.2.10; http://www.ncbi.nlm.nih.gov/blast/Blast.cgi).

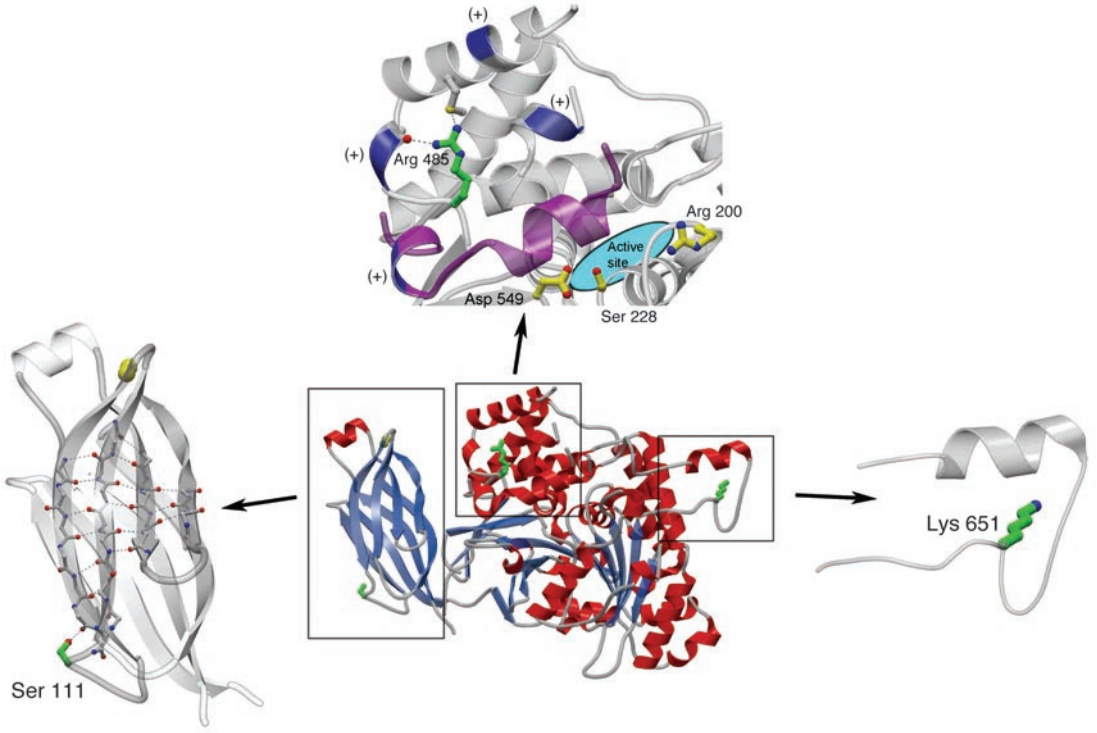

Figure 8
cPLA$_{2\alpha}$ tertiary structure and location of amino acid substitutions. The cPLA$_{2\alpha}$ structure is depicted as a ribbon diagram with α-helices in red, β-strands as blue arrows, loops in gray, and Ca^{2+} ions as yellow spheres (center). The locations of described amino acid side-chain substitutions are highlighted in green. Three magnified views highlight each mutation. In the left panel, the Ca^{2+} binding domain is highlighted and shows the S111 position. The upper panel shows that the catalytic domain contains an active site composed of the catalytic dyad of Ser228 and Asp549. Arg200 is also required for catalytic activity (functionally obligate amino acids are shown with yellow carbon atoms and bonds) (11). Arg485 is in proximity to a cluster of lysine residues (blue) that are essential for interfacial binding of cPLA$_{2\alpha}$ (12) and for binding PIP_2 (13). p.[R485] is located in a cleft in a helical region containing several positively charged residues in the membrane-facing region of the catalytic domain (11), where the side-chain guanido group forms 2 stabilizing hydrogen-bonding interactions within this fold. A "hinged lid," which prevents exposure of the active site to substrate until interaction with a lipid membrane is shown in purple. The right panel depicts the location of Lys651, the relative position of which has not been determined.

of their biosynthesis and with the expected intermediate reduction in biosynthesis in the family members who are heterozygous for a single mutant allele. Each of the amino acids affected by the mutations is conserved across species.

The cPLA$_{2\alpha}$ gene (*PLA2G4A*; OMIM 600522) consists of 18 exons in 164 k base pairs mapped to chromosome locus 1q25 (14) and encodes a 749–amino acid protein. Catalytic activity is regulated by physiologic levels of intracellular calcium concentrations and phosphorylation (15–18) and enhanced by PIP_2 (19) and ceramide 1–phosphate (20). When activated, the enzyme translocates from the cytoplasm to bilayer lipid membranes where it binds and preferentially hydrolyzes AA from the *sn*-2 position of phospholipid substrate to release free AA and lysophospholipid (21–23). Two distinct functional domains of cPLA$_{2\alpha}$ have been described: a calcium-binding domain and a catalytic domain (24).

Our results indicate that the patient inherited 2 different cPLA$_{2\alpha}$ alleles: one p.[S111P] rare variant allele from his mother and a combined p.[R485H] (rare variant) and p.[K651R] SNP allele from his father. Each of the 3 transitions encodes an amino acid substitution in regions of the cPLA$_{2\alpha}$ protein that are highly conserved across species (Figure 7B). The crystal structure of cPLA$_{2\alpha}$ elucidates the location of the variant amino acids and chemical interactions of the amino acid side chains. (Figure 8).

Although small intestinal ulcers unrelated to use of NSAIDs or enteric-coated drugs are uncommon, a number of such patients have been reported (1). cPLA$_{2\alpha}$ deficiency may be considered in the molecular differential diagnosis of such ulcers, particularly those with onset early in life. Technical advances, such as video capsule endoscopy, have recently provided means to detect heretofore undiscovered small intestinal lesions, and recent studies suggest that small intestinal mucosal breaks are not uncommon among NSAID users and to a lesser degree in nonusers (2, 3, 25). The late onset of severe bleeding in this patient may reflect an age-dependent risk of platelet inhibition, as the bleeding risk of aspirin use is low in young individuals but increases with age (26).

Nonselective COX inhibition by NSAIDs causes gastroduodenal ulceration with high morbidity and mortality (27) as well as the generally more subtle but frequent ulceration of the jejunum and ileum (2). In contrast, this patient with cPLA$_{2\alpha}$ deficiency suffered from severe ulcer disease exclusively of the ileum and jejunum; no gastroduodenal ulcers had been detected on repeated upper intestinal endoscopies. This restriction of ulcer disease to the jejunum and ileum has been characteristic of other reported patients with NSAID-independent small intestinal ulcers (1, 3). The selectivity of the jejunum and ileum could result from cPLA$_{2\alpha}$ serving as the key phospholipase providing AA substrate in these portions of the

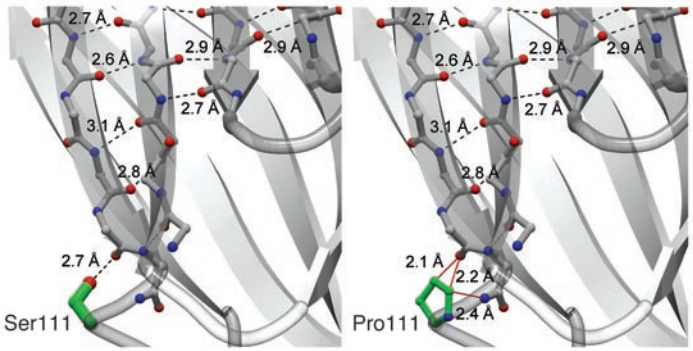

Figure 9

Effects of proline substitution at residue 111 of $cPLA_{2\alpha}$. Comparison of the wild-type $cPLA_{2\alpha}$ structure (left) with a model of the p.[S111P] mutation (right). Backbone carbon atoms are shown in gray, oxygen atoms and hydroxy groups in red, nitrogen atoms in blue, and side-chain carbon atoms of the 111 position in green. Hydrogen-bonding interactions are shown in dashed black lines and sterically unfavorable close distances are shown in solid red lines. A hydrogen-bonding interaction has an ideal distance of 2.7–3.0 Å between oxygen and nitrogen-hydrogen–bond donors and acceptors and an ideal distance of 3.1–3.2 Å for sulfur to nitrogen-hydrogen–bond donors and acceptors. Nonbonded distances smaller than 2.5 Å between nitrogen and oxygen-hydrogen–bonding donors and acceptors are sterically and energetically unfavorable and are generally not observed in nature. Distances longer than 3.5 Å do not contribute favorable energy toward folding stabilization. Modeling of proline in position 111 reveals that 1 ideal hydrogen-bonding interaction of 2.7 Å between the p.[S111] side-chain hydroxyl moiety and the backbone carbonyl group of p.[T108] has been replaced by 3 sterically unfavorable interactions (<2.5 Å). Two of these unfavorable interactions lie between the hydrophobic proline Cγ and Cδ atoms and the p.[T108] carbonyl, while 1 unfavorable interaction is between the proline Cδ and the amide nitrogen of p.[S111]. The p.[S111P] mutation is predicted to cause unfavorable interactions (red lines) in the absence of a structural rearrangement of the protein. The predicted decrease in stability of the adjacent β-strands likely affects the entire Ca^{2+}-binding domain.

small intestine in contrast with a different phospholipase releasing AA for biosynthesis of the PGs that protect the stomach (28, 29) and duodenum from ulceration. Alternatively, lipoxygenase-derived products of AA may be more important contributors to ulcer formation in the stomach and duodenum than in the ileum and jejunum. LTB_4 concentrations were markedly increased in the fundic mucosa of rats that received indomethacin compared with controls, and 5-lipoxygenase inhibitors have been shown to mitigate NSAID-induced gastric and intestinal lesions (30). Notably, this attenuation was more profound in gastric mucosa, which demonstrated 95.4% and 98.8% reductions in lesion number and size, respectively, compared with 72.5% and 86.9% reductions in the small intestine. The finding of jejunoileal ulcers as a phenotype of $cPLA_{2\alpha}$ deficiency identifies a signaling pathway linked to this disease and affords a hypothesis that loss of function at other steps in the pathway could yield a similar phenotype. The small intestinal sequelae of $cPLA_{2\alpha}$ deficiency also becomes relevant in consideration of the consequences of employing selective $cPLA_{2\alpha}$ inhibitors as therapeutic agents.

A concerted body of evidence indicates that $cPLA_{2\alpha}$ is the principal and rate-limiting phospholipase responsible for initiating eicosanoid biosynthesis in the platelet (31–34). Our findings strongly support the concept that in the intact platelet, $cPLA_{2\alpha}$ initiates the signaling-induced release of virtually all of the AA that is substrate for both the COX-1 and 12-lipoxygenase–derived pathways. Analysis of eicosanoid biosynthesis in activated platelets, therefore, provides an optimal biochemical phenotype with which to detect heterozygosity (Figure 3). LTB_4 biosynthesis by blood leukocytes also is derived almost entirely via the $cPLA_{2\alpha}$ pathway.

When platelet lysates are studied instead of intact physiologically activated platelets, a minor phospholipase activity is detected from the described patient's platelets. This residual phospholipase activity in disrupted cells may reflect a different phospholipase that does not participate in physiologic signaling (e.g., secretory PLA_2 [$sPLA_2$]), or alternatively, the variant $cPLA_{2\alpha}$ in the disrupted cell may access the synthetic substrate in a way that would not occur during signaling in an intact cell that requires translocation of the enzyme from cytoplasm to lipid membrane and a controlled interaction with that membrane. The finding of decreased quantity of $cPLA_{2\alpha}$ protein in sonicated platelets suggests either decreased expression or increased degradation of one or both of the 2 allelic variants.

The complete loss of ADP-induced dense granule release in the $cPLA_{2\alpha}$-deficient platelet is consistent with the key participation of TxA_2 in this response to ADP signaling (35, 36). The observed granule release and normal shape change by the patient's platelets in response to collagen, however, indicates that dense granules are at least present and that initial aggregatory shape change mechanisms are intact in the patient's platelets. These findings predict that selective inhibition of $cPLA_{2\alpha}$ in humans would have an aspirin-like antiplatelet effect. The excretion of 11-dTxB_2 at 16% of normal levels suggests that TxA_2 biosynthesis in some nonplatelet cell(s) proceeds via another phospholipase.

The roles of eicosanoids in malignancy are significant, complex, and incompletely understood (37), making prediction of the consequences of the deficiency of $cPLA_{2\alpha}$ with regard to tumorigenesis difficult. This complexity has been highlighted in experimental models with $cPLA_{2\alpha}$-deficient mice. For example, $cPLA_{2\alpha}$-deficient mice demonstrated a decrease in colon tumor number and size when crossed with Apc^{Min} mice (38). However, when $cPLA_{2\alpha}$-null mice were challenged with azoxymethane, they universally developed colon tumors as opposed to a significantly lower number among control mice (39). Although the association between $cPLA_{2\alpha}$ deficiency and renal-cell carcinoma may be coincidental, further exploration of this relationship may provide clues to the mechanistic involvement of $cPLA_{2\alpha}$ and downstream eicosanoids in neoplastic disease.

$CPLA_{2\alpha}$ (–/–) mice (35, 40–44) manifest platelet dysfunction and have small bowel ulcers that are much less severe than in the patient lacking this enzyme. These knockout mice have cardiac hypertrophy, which is not evident in the patient. Renal-cell carcinoma has not been reported in these mice, which do manifest reproductive abnormalities and are resistant to cerebral ischemic injury and inflammatory arthritis.

Collectively, the findings reported here indicate that $cPLA_{2\alpha}$ provides substrate for virtually all of the biosynthesis of eicosanoids by the platelets, by circulating leukocytes, and by the cells from which the cysteinyl leukotrienes are derived. Moreover, $cPLA_{2\alpha}$ contributes importantly to the eicosanoid biosynthesis responsible for maintenance of the integrity of the small intestine. The patient's improvement with administration of the PGE analogue

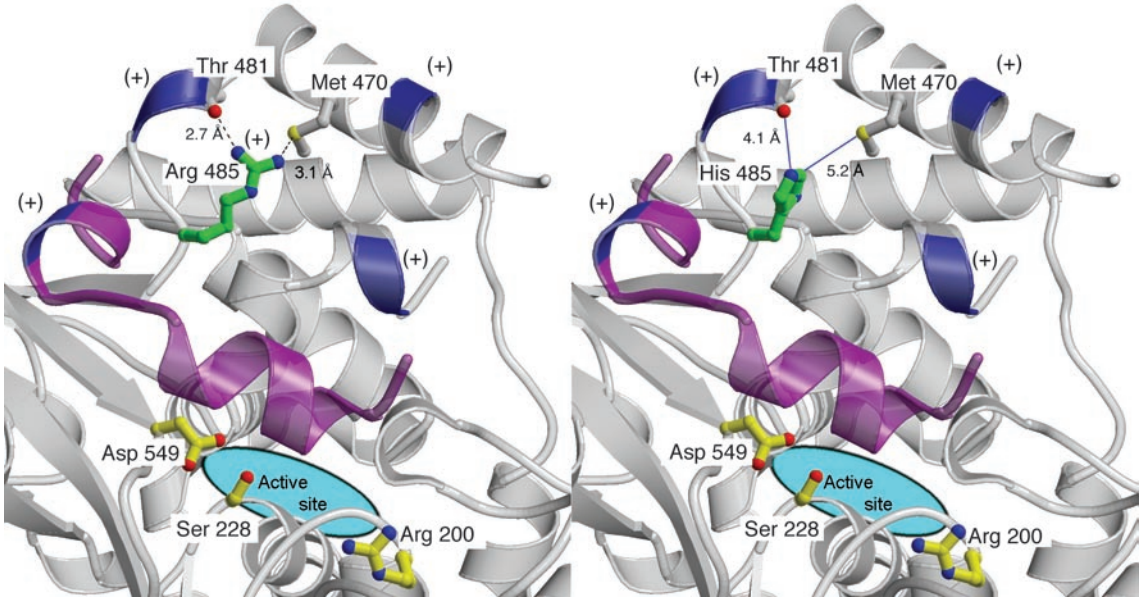

Figure 10
Effects of histidine substitution at residue 485 of $cPLA_{2\alpha}$. Comparison of the wild-type $cPLA_{2\alpha}$ structure (left) with a model of the p.[R485H] mutation (right). Backbone trace is shown in gray with the backbone of positively charged positions shown in blue and labeled with a plus sign; the capping helix is highlighted in purple. Oxygen atoms and hydroxy groups are shown in red, nitrogen atoms in blue, and sulfur atoms in yellow. The side-chain carbon atoms of the 485 position are shown in green, and the side-chain atoms of catalytically important residues are highlighted in yellow. Hydrogen bonds are indicated with a dashed black line while distances too long to form a hydrogen-bonding interaction are shown with solid blue lines. Modeling of histidine into position 485 reveals that 2 ideal hydrogen bonds between the side chain of p.[R485] and the backbone carbonyl of p.[T481] and side-chain $S\gamma$ of p.[M470] are lost. This mutation is predicted to introduce a destabilizing cavity in the location of the p.[R485] side chain.

misoprostol suggests that the contribution of $cPLA_{2\alpha}$ is in providing PGE_2 to the small intestine and that the ulcers are not solely due to the absence of eicosanoid biosynthesis in the platelets and leukocytes. Other phospholipases must account for biosynthesis of TxA_2 and prostanoids in many other cells in the body because urinary metabolites of TxA_2 and the prostanoids are only partially reduced in the absence of $cPLA_{2\alpha}$.

In conclusion, we have characterized compound heterozygous $cPLA_{2\alpha}$ variants that cause platelet dysfunction and are associated with multiple recurrent small bowel ulcers. Characterization of this deficiency has the potential for elucidating the biology and pathophysiology of $cPLA_{2\alpha}$. These findings also have significant implications for the safety and effectiveness of pharmacologic inhibition of the $cPLA_{2\alpha}$ enzyme.

Methods

Study conduct. Informed consent was obtained from all participants after study approval by the Vanderbilt University Institutional Review Board. The patient was admitted to the General Clinical Research Center at Vanderbilt University Medical Center for 7 days, during which all medications were held. Consecutive 24-hour urine collections were obtained prior to phlebotomy, which was subsequently performed daily after an overnight fast. Blood specimens from family members were obtained remotely and shipped to our facility. Healthy male volunteers who were prospectively requested not to take NSAIDs or other medications for the preceding 2 weeks served as controls.

Urinary metabolites of PGE_2, PGD_2, PGI_2, and TxA_2. 11-dTxB$_2$, PGI-M, PGD-M, and PGE-M were assayed using MS (6–8, 45) from separate 24-hour urine collections on different days.

Platelet-derived (serum) TxB_2 and 12-HETE. Blood from the patient on multiple days was drawn into a glass container and allowed to clot by incubating at 37°C for 45 minutes. The serum layer was collected after centrifugation, and TxB_2 was assayed by gas chromatography/electron capture ionization/MS (GC/ECI/MS) (46, 47). 12-HETE was assayed by liquid chromatography (LC)/atmospheric pressure chemical ionization/MS/MS using a silica HPLC column (48).

Urinary LTE_4. LTE_4 was analyzed by a previously published LC/MS/MS method (49) with minor modifications.

Whole-blood LTB_4. Venous blood was drawn into standard heparinized phlebotomy tubes, and $CaCl_2$ (0.5 mM) and $MgCl_2$ (0.5 mM) were added. Blood was activated with a calcium ionophore, A23187 (0.05 mM), incubated at 37°C for 45 minutes, and centrifuged at 2000 *g* for 5 minutes; supernatant was stored at –80°C until analyzed by LC/electrospray ionization/MS/MS. 200-μl aliquots of thawed sample were extracted with hexane/ethyl acetate (1:1) after addition of [$^2H_4$] LTB_4 (2 ng) (Cayman Chemical) as an internal standard. The samples were then dried and resuspended in 30% acetonitrile (ACN). Levels of LTB_4 were determined by LC/electrospray ionization/MS/MS using selected reaction monitoring on a Finnigan TSQ Quantum system (Finnigan Corp.). Reverse-phase HPLC (Phenomenex Jupiter ODS [5 μm], 2 mm × 150 mm; C18 300 Å column) was performed with a gradient starting with 30% ACN, holding for 2 minutes, followed by a linear gradient increasing to 100% ACN/acetic acid (0.05%) over 4 minutes and held for an additional 4 minutes. The flow rate was 200 μl/min. Under these conditions, the internal standard eluted in 7.7 minutes. The mass spectrometer was operated in negative-ion mode. Nitrogen was used as the sheath gas (30 mTorr) and auxiliary gas (14 mTorr) to assist the nebulization. The heated capillary was operated at 200°C and 20 V, and the tube lens voltage was set at –138 V. Ions were subjected to collision-

induced dissociation at an argon pressure of 1.5 mTorr. Mass transition ions monitored at 22.0 eV were *m/z* 335 to 195 for [$^2H_4$] LTB_4 and 339 to 197 for [$^2H_0$] LTB_4. Data acquisition and analysis were performed using XCaliber software, version 1.3.

TxB_2 production in washed platelets. Platelets were gel filtered (50), and 100 μl of the platelet suspension (600,000 cells/μl) was incubated with [$^2H_8$] AA (2 μM) at 37°C for 15 minutes. After stopping the reaction, TxB_2 was purified, derivatized, and analyzed by GC/ECI/MS.

Immunoblotting of $cPLA_{2\alpha}$ protein. Western blot analysis of protein was performed using rabbit anti-$cPLA_2$ (Cell Signaling Technology) or goat anti-actin (Santa Cruz Biotechnology Inc.) primary antibodies and horseradish peroxidase–coupled secondary antibodies (Santa Cruz Biotechnology Inc.). Band intensity was quantified using image analysis software (Quantity One, v. 4.3.1, Bio-Rad).

Platelet aggregation. Citrated PRP from peripheral venous blood from the patient and control volunteers was used to assess turbidimetric platelet aggregation induced by ADP, collagen, or AA. Platelet counts were adjusted to 2.6 to 2.8 × 10^8 cells/ml prior to aggregation. Simultaneous ATP secretion was quantified by monitoring luminescence produced by luciferase using an optical platelet aggregometer (Chronolog).

Lymphoblast separation and culture. Lymphoblasts were separated from whole blood using LymphoSep lymphocyte separation medium (MP Biochemicals) and cultured after addition of cyclosporine per manufacturer's instructions.

PLA_2 activity. Platelets obtained on 2 different days from the patient and from 2 volunteers were frozen as PRP in citrate at –80°C. Thawed platelets or fresh-cultured lymphoblasts were washed and resuspended in buffer (10 mM HEPES, 0.34 M sucrose, 10% glycerol, 1 mM EDTA, pH 7.75) with a protease inhibitor cocktail of antipain, aprotinin, chymostatin, leupeptin, and pepstatin (each 1 μg/ml). Whole-cell lysate was obtained by sonication of cell suspension followed by brief centrifugation at 10,000 *g*. Dithiothreitol (1 mM) was added to prevent oxidative enzyme degradation. PLA_2 activity was measured from whole-cell lysate (50 μg protein) with a radiolabeled substrate, l-3-phosphatidylcholine, 1-stearoyl-2-[1-^{14}C] arachidonyl (^{14}C-SAPC; 450 pmol, 55,000 dpm) under conditions described by Leslie and Gelb (51) (150 mM NaCl, 1 mg/ml BSA, 42 mM HEPES, 10 mM $CaCl_2$, pH 7.5). Substrate hydrolysis was measured over 30 minutes, demonstrating linear kinetics. Reactions were stopped by addition of chloroform/methanol (2:1), and the extracted lipids were separated by thin-layer chromatography. Residual substrate and hydrolyzed AA were quantified by analyzing radioactivity using a Bioscan AR-200 imaging scanner.

$cPLA_{2\alpha}$ cDNA sequencing. Oligonucleotide primer sequences are listed in Supplemental Table 1 (supplemental material available online with this article; doi:10.1172/JCI30473DS1). cDNA was obtained by reverse transcription (Invitrogen Superscript III and Elongase kits) using total RNA isolated with a whole-blood RNA collection system (QIAGEN PAXgene) as a template and oligo dT as a primer. Following RT-PCR amplification using primer 1 and primer 2 oligonucleotide primers, DNA sequencing was done using primers 1–14 with Applied Biosystems BigDye, v. 3.1.

$cPLA_{2\alpha}$ genomic DNA sequencing. The 18 exons of the *PLA2G4A* gene were PCR amplified from genomic DNA, using sequence-specific primers. PCR reactions were performed with AmpliTaq Gold (Applied Biosystems), 10X PCR buffer (Applied Biosystems), and dNTP mix (New England Biolabs Inc.), using the PCR Express (Hybaid). PCR products were sequenced by the Vanderbilt University DNA Sequencing Facility using BigDye Terminator chemistry v. 3.1 (Applied Biosystems) on an ABI 3730xl automated sequencer and analyzed using DNA Sequencing Analysis 5.0 software (Applied Biosystems).

Population polymorphism screening. Genotyping for 3 identified $cPLA_{2\alpha}$ variants was performed using an allelic discrimination assay with the ABI PRISM 7900HT Sequence Detection System (Applied Biosystems) using Assays-On-Demand (hCV16195860) for c.[1952A>G] or Assays-By-Design for c.[331T>C] and c.[1454G>A] following the manufacturer's instructions. Amplification was performed in a 384-well DNA Engine Tetrad 2 Peltier Thermal Cycler (MJ Research) under the following conditions: 94°C, 10 min; 92°C, 15 s; 60°C, 1 min (70 cycles); 4°C, hold. Systematic genotyping errors were minimized by use of a system of quality control checks with duplicated samples (52). Genomic DNA from the patient and family members was obtained from whole-blood or lymphoblast cultures. 368 DNA samples from 4 ethnically diverse panels (white, African American, Hispanic, and Han Chinese) were purchased from the Coriell Institute, and 50 Italian DNA samples were a gift from Ornella Semino (University of Pavia, Pavia, Italy).

Molecular modeling. Computer-simulated modeling of the $cPLA_{2\alpha}$ protein and the identified amino acid substitutions was performed using the program O (53). Ribbon diagram figures were made using MOLSCRIPT (54) and RASTER3D (55). Structural data was obtained from the RCSB Protein Data Bank (http://www.pdb.org; PDB ID: 1CJY) (56, 57).

Statistics. Normally distributed continuous variables were compared using a 2-sided unpaired *t* test with Welch's correction applied when variances were different. Mann-Whitney *U* test was used for comparison of continuous variables without normal distribution. PLA_2 activity was compared using 2-way ANOVA. Reference ranges were calculated as mean ± 2 SDs. The 0.025 quantiles for serum TxB_2 and for serum 12-HETE were calculated by the Harrell-Davis method (58). Means are reported ± SD unless otherwise specified.

Acknowledgments

We would like to thank our patient and his family for their ongoing cooperation with this investigation, Taneem Amin for his technical assistance, Jeffrey A. Canter for his assistance, and Ornella Semino (University of Pavia, Pavia, Italy) for the generous donation of DNA samples. We thank Frank Harrell for his assistance with statistical analysis. This work was supported in part by NIH grants HL81009, GM15431, HL65962, and RR00095.

Received for publication September 26, 2006, and accepted in revised form March 12, 2008.

Address correspondence to: John A. Oates, Vanderbilt University Medical Center, Department of Internal Medicine, Clinical Pharmacology Division, 536 Robinson Research Bldg., 2222 Pierce Ave., Nashville, Tennessee 37232-6602, USA. Phone: (615) 343-4847; Fax: (615) 343-9446; E-mail: john.oates@vanderbilt.edu.

1. Matsumoto, T., et al. 2004. Non-specific multiple ulcers of the small intestine unrelated to non-steroidal anti-inflammatory drugs. *J. Clin. Pathol.* **57**:1145–1150.
2. Maiden, L., et al. 2005. A quantitative analysis of NSAID-induced small bowel pathology by capsule enteroscopy. *Gastroenterology.* **128**:1172–1178.
3. Goldstein, J.L., et al. 2005. Video capsule endoscopy to prospectively assess small bowel injury with celecoxib, naproxen plus omeprazole, and placebo. *Clin. Gastroenterol. Hepatol.* **3**:133–141.
4. Brodie, D.A., Cook, P.G., Bauer, B.J., and Dagle, G.E. 1970. Indomethacin-induced intestinal lesions in the rat. *Toxicol. Appl. Pharmacol.* **17**:615–624.
5. Lu, Y.F., Mizutani, M., Neya, T., and Nakayama, S. 1995. Indomethacin-induced lesion modifies contractile activity in rat small intestines. *Scand. J. Gastroenterol.* **30**:445–450.
6. Morrow, J.D., and Minton, T.A. 1993. Improved assay for the quantification of 11-dehydrothromboxane B2 by gas chromatography-mass spectrometry. *J. Chromatogr.* **612**:179–185.
7. Morrow, J.D., et al. 1991. Quantification of the major urinary metabolite of prostaglandin D2 by a stable isotope dilution mass spectrometric assay. *Anal. Biochem.* **193**:142–148.
8. Murphey, L.J., et al. 2004. Quantification of the major urinary metabolite of PGE2 by a liquid chromatographic/mass spectrometric assay: determination of cyclooxygenase-specific PGE2 synthesis in

healthy humans and those with lung cancer. *Anal. Biochem.* **334**:266–275.
9. Nakayama, T., et al. 2002. Splicing mutation of the prostacyclin synthase gene in a family associated with hypertension. *Biochem. Biophys. Res. Commun.* **297**:1135–1139.
10. Patrono, C., Garcia Rodriguez, L.A., Landolfi, R., and Baigent, C. 2005. Low-dose aspirin for the prevention of atherothrombosis. *N. Engl. J. Med.* **353**:2373–2383.
11. Dessen, A. 2000. Structure and mechanism of human cytosolic phospholipase A2. *Biochim. Biophys. Acta.* **1488**:40–47.
12. Das, S., and Cho, W. 2002. Roles of catalytic domain residues in interfacial binding and activation of group IV cytosolic phospholipase A2. *J. Biol. Chem.* **277**:23838–23846.
13. Six, D.A., and Dennis, E.A. 2003. Essential Ca(2+)-independent role of the group IVA cytosolic phospholipase A(2) C2 domain for interfacial activity. *J. Biol. Chem.* **278**:23842–23850.
14. Tay, A., et al. 1995. Cytosolic phospholipase A2 gene in human and rat: chromosomal localization and polymorphic markers. *Genomics.* **26**:138–141.
15. Gronich, J.H., Bonventre, J.V., and Nemenoff, R.A. 1988. Identification and characterization of a hormonally regulated form of phospholipase A2 in rat renal mesangial cells. *J. Biol. Chem.* **263**:16645.
16. Gijon, M.A., Spencer, D.M., Kaiser, A.L., and Leslie, C.C. 1999. Role of Phosphorylation Sites and the C2 Domain in Regulation of Cytosolic Phospholipase A2. *J. Cell Biol.* **145**:1219–1232.
17. Das, S., Rafter, J.D., Kim, K.P., Gygi, S.P., and Cho, W. 2003. Mechanism of Group IVA Cytosolic Phospholipase A2 Activation by Phosphorylation. *J. Biol. Chem.* **278**:41431–41442.
18. Leslie, C.C. 1997. Properties and Regulation of Cytosolic Phospholipase A2. *J. Biol. Chem.* **272**:16709–16712.
19. Mosior, M., Six, D.A., and Dennis, E.A. 1998. Group IV cytosolic phospholipase A2 binds with high affinity and specificity to phosphatidylinositol 4,5-bisphosphate resulting in dramatic increases in activity. *J. Biol. Chem.* **273**:2184–2191.
20. Pettus, B.J., et al. 2004. Ceramide 1-phosphate is a direct activator of cytosolic phospholipase A2. *J. Biol. Chem.* **279**:11320–11326.
21. Clark, J.D., et al. 1991. A novel arachidonic acid-selective cytosolic PLA2 contains a Ca(2+)-dependent translocation domain with homology to PKC and GAP. *Cell.* **65**:1043–1051.
22. Schievella, A.R., Regier, M.K., Smith, W.L., and Lin, L.-L. 1995. Calcium-mediated Translocation of Cytosolic Phospholipase A(2) to the Nuclear Envelope and Endoplasmic Reticulum. *J. Biol. Chem.* **270**:30749–30754.
23. Peters-Golden, M., Song, K., Marshall, T., and Brock, T. 1996. Translocation of cytosolic phospholipase A2 to the nuclear envelope elicits topographically localized phospholipid hydrolysis. *Biochem. J.* **318**:797–803.
24. Nalefski, E.A., et al. 1994. Delineation of 2 functionally distinct domains of cytosolic phospholipase A2, a regulatory Ca(2+)-dependent lipid-binding domain and a Ca(2+)-independent catalytic domain. *J. Biol. Chem.* **269**:18239–18249.
25. Liangpunsakul, S., Chadalawada, V., Rex, D.K., Maglinte, D., and Lappas, J. 2003. Wireless capsule endoscopy detects small bowel ulcers in patients with normal results from state of the art enteroclysis. *Am. J. Gastroenterol.* **98**:1295–1298.
26. Garcia Rodriguez, L.A., Hernandez-Diaz, S., and de Abajo, F.J. 2001. Association between aspirin and upper gastrointestinal complications: systematic review of epidemiologic studies. *Br. J. Clin. Pharmacol.* **52**:563–571.
27. Wolfe, M.M., Lichtenstein, D.R., and Singh, G. 1999. Gastrointestinal toxicity of nonsteroidal antiinflammatory drugs. *N. Engl. J. Med.* **340**:1888–1899.
28. Masuda, S., Murakami, M., Ishikawa, Y., Ishii, T., and Kudo, I. 2005. Diverse cellular localizations of secretory phospholipase A2 enzymes in several human tissues. *Biochim. Biophys. Acta.* **1736**:200–210.
29. Ni, Z., Okeley, N.M., Smart, B.P., and Gelb, M.H. 2006. Intracellular actions of group IIA secreted phospholipase A2 and group IVA cytosolic phospholipase A2 contribute to arachidonic acid release and protaglandin production in rat gastric mucosal cells and transfected human embryonic kidney cells. *J. Biol. Chem.* **281**:16245–16255.
30. Rainsford, K.D. 1999. Inhibition by leukotriene inhibitors, and calcium and platelet-activating factor antagonists, of acute gastric and intestinal damage in arthritic rats and in cholinomimetic-treated mice. *J. Pharm. Pharmacol.* **51**:331–339.
31. Kramer, R.M., Roberts, E.F., Manetta, J.V., Hyslop, P.A., and Jakubowski, J.A. 1993. Thrombin-induced phosphorylation and activation of Ca(2+)-sensitive cytosolic phospholipase A2 in human platelets. *J. Biol. Chem.* **268**:26796–26804.
32. Bartoli, F., et al. 1994. Tight binding inhibitors of 85-kDa phospholipase A2 but not 14-kDa phospholipase A2 inhibit release of free arachidonate in thrombin-stimulated human platelets. *J. Biol. Chem.* **269**:15625–15630.
33. Coffey, M.J., et al. 2004. Interactions of 12-lipoxygenase with phospholipase A2 isoforms following platelet activation through the glycoprotein VI collagen receptor. *FEBS Lett.* **576**:165–168.
34. Wong, D.A., Kita, Y., Uozumi, N., and Shimizu, T. 2002. Discrete Role for Cytosolic Phospholipase A2{alpha} in Platelets: Studies Using Single and Double Mutant Mice of Cytosolic and Group IIA Secretory Phospholipase A2. *J. Exp. Med.* **196**:349–357.
35. Best, L.C., Holland, T.K., Jones, P.B., and Russell, R.G. 1980. The interrelationship between thromboxane biosynthesis, aggregation and 5-hydroxytryptamine secretion in human platelets in vitro. *Thromb. Haemost.* **43**:38–40.
36. Rand, M.L., et al. 1996. Conditions influencing release of granule contents from human platelets in citrated plasma induced by ADP or the thrombin receptor activating peptide SFLLRN: direct measurement of percent release of beta-thromboglobulin and assessment by flow cytometry of P-selectin expression. *Am. J. Hematol.* **52**:288–294.
37. Wang, D., Mann, J.R., and Dubois, R.N. 2005. The role of prostaglandins and other eicosanoids in the gastrointestinal tract. *Gastroenterology.* **128**:1445–1461.
38. Hong, K.H., et al. 2001. Deletion of cytosolic phospholipase A2 suppresses ApcMin-induced tumorigenesis. *Proc. Natl. Acad. Sci. U. S. A.* **98**:3935–3939.
39. Ilsley, J.N.M., et al. 2005. Cytoplasmic Phospholipase A2 Deletion Enhances Colon Tumorigenesis. *Cancer Res.* **65**:2636–2643.
40. Bonventre, J.V. 1999. The 85-kD cytosolic phospholipase A2 knockout mouse: a new tool for physiology and cell biology. *J. Am. Soc. Nephrol.* **10**:404–412.
41. Bonventre, J.V., et al. 1997. Reduced fertility and postischaemic brain injury in mice deficient in cytosolic phospholipase A2. *Nature.* **390**:622.
42. Sapirstein, A., and Bonventre, J.V. 2000. Specific physiological roles of cytosolic phospholipase A2 as defined by gene knockouts. *Biochim. Biophys. Acta.* **1488**:139–148.
43. Haq, S., et al. 2003. Deletion of cytosolic phospholipase A2 promotes striated muscle growth. *Nat. Med.* **9**:944–951.
44. Bonventre, J.V. 2004. Cytosolic phospholipase A2[alpha] reigns supreme in arthritis and bone resorption. *Trends Immunol.* **25**:116.
45. Daniel, V.C., Minton, T.A., Brown, N.J., Nadeau, J.H., and Morrow, J.D. 1994. Simplified assay for the quantification of 2,3-dinor-6-keto-prostaglandin F1 alpha by gas chromatography-mass spectrometry. *J. Chromatogr. B Biomed. Appl.* **653**:117–122.
46. FitzGerald, G.A., Healy, C., and Daugherty, J. 1987. Thromboxane A2 biosynthesis in human disease. *Fed. Proc.* **46**:154–158.
47. FitzGerald, G.A., et al. 1983. Aspirin inhibits endogenous prostacyclin and thromboxane biosynthesis in man. *Adv. Prostaglandin Thromboxane Leukot. Res.* **11**:265–266.
48. Yin, H., Porter, N.A., and Morrow, J.D. 2005. Separation and identification of F2-isoprostane regioisomers and diastereomers by novel liquid chromatographic/mass spectrometric methods. *J. Chromatogr. B Analyt. Technol. Biomed. Life Sci.* **827**:157–164.
49. Mizugaki, M., Hishinuma, T., and Suzuki, N. 1999. Determination of leukotriene E4 in human urine using liquid chromatography-tandem mass spectrometry. *J. Chromatogr. B Biomed. Sci. Appl.* **729**:279–285.
50. Boutaud, O., Aronoff, D.M., Richardson, J.H., Marnett, L.J., and Oates, J.A. 2002. Determinants of the cellular specificity of acetaminophen as an inhibitor of prostaglandin H(2) synthases. *Proc. Natl. Acad. Sci. U. S. A.* **99**:7130–7135.
51. Leslie, C.C., and Gelb, M.H. 2004. Assaying phospholipase A2 activity. *Methods Mol. Biol.* **284**:229–242.
52. Rimmler, J., et al. 1998. Development of a data coordinating center (DCC): data quality control for complex disease studies. *Am. J. Hum. Genet. Suppl.* **63**:A240.
53. Jones, T.A., Zou, J.Y., Cowan, S.W., and Kjeldgaard, M. 1991. Improved methods for building protein models in electron density maps and the location of errors in these models. *Acta Crystallogr. A.* **47**:110–119.
54. Kraulis, P.J. 1991. MOLSCRIPT — a program to produce both detailed and schematic plots of protein structures. *J. Appl. Cryst.* **24**:946–950.
55. Merritt, E.A., and Murphy, M.E.P. 1994. Raster3D Version 2.0 — a program for photorealistic molecular graphics. *Acta Crystallogr. D Biol. Crystallogr.* **50**:869–873.
56. Berman, H.M., et al. 2000. The Protein Data Bank. *Nucl. Acids Res.* **28**:235–242.
57. Dessen, A., et al. 1999. Crystal structure of human cytosolic phospholipase A2 reveals a novel topology and catalytic mechanism. *Cell* **97**:349–360.
58. Harrell, F.E., and Davis, C.E. 1982. A new distribution-free quantile estimator. *Biometrika.* **69**:635–640.
59. Tatusova, T.A., and Madden, T.L. 1999. BLAST 2 sequences, a new tool for comparing protein and nucleotide sequences. *FEMS Microbiol. Lett.* **174**:247–250.